Asian Journal of Chemical Sciences

2(4): 1-11, 2017; Article no.AJOCS.32615
ISSN: 2456-7795

XRD Studies, Spectral Characteristics, TGA and DFT of 2,4-Diamino-6-phenyl-1,3,5-triazine: Phenylthioacetic Acid Cocrystal

S. Kumaresan[1*], V. Velmurugan[2], P. Palanisamy[3], N. Bhuvanesh[4], R. Subramanian[5], V. S. Pradosh[6] and P. Ramkumar[6]

[1]Department of Biotechnology, Manonmaniam Sundaranar University, Tirunelveli–627 012, Tamilnadu, India.
[2]Department of Chemistry, Manonmaniam Sundaranar University, Tirunelveli–627 012, Tamilnadu, India.
[3]Department of Chemistry, Pioneer Kumaraswamy College, Nagercoil–629 003, Tamilnadu, India.
[4]Department of Chemistry, Texas A&M University, College Station, Texas–7784, USA.
[5]Centre for Scientific and Applied Research, PSN College of Engineering and Technology, Melathediyoor, Tirunelveli- 627152, Tamilnadu, India.
[6]Department of Chemistry, Noorul Islam University, Kumaracoil, Thuckalay–629 180, Tamilnadu, India.

Authors' contributions

This work was prepared in the research group of author SK. He proposed the work and drafted the manuscript. Authors VV and PP participated in the design, conduct of the experiments and collected data. All authors read and approved the final manuscript.

Article Information

DOI: 10.9734/AJOCS/2017/32615
Editor(s):
(1) Georgiy B. Shul'pin, Semenov Institute of Chemical Physics, Russian Academy of Sciences, Moscow, Russia.
Reviewers:
(1) Birsa Mihail Lucian, Alexandru Ioan Cuza University of Iasi, Romania.
(2) Marta Łaszcz, Pharmaceutical Research Institute (PRI), Poland.
(3) Larbah Youssef, Nuclear Research Centre of Alger, Algeria.
Complete Peer review History: http://prh.sdiarticle3.com/review-history/20138

Original Research Article

Received 4th March 2017
Accepted 13th June 2017
Published 20th July 2017

ABSTRACT

The title compound was prepared crystallizing together the co-formers namely, 2,4-diamino-6-phenyl-1,3,5-triazine (DAPT) and phenylthioacetic acid (PTAA) in methanol. The compound crystallized in the orthorhombic space group $Pca2_1$ with a = 12.384(2) Å, b = 18.698 (3) Å, c = 7.0428(11) Å, V = 1630.8(5) Å^3, and Z = 4. The compound existed as a 1:1 cocrystal. The dihedral

**Corresponding author: E-mail: skumarmsu@yahoo.com, skumarmsu@gmail.com;*

angle between the two formers is 50.89(9)°. The primary and secondary interactions between DAPT and PTAA form two different discrete chains C(3) that link the DAPT ribbons in adjacent layer. Mass spectra indicate the transfer of a carboxylic acid proton to form PTAA to the nitrogen of DAPT.

Keywords: Molecular cocrystal; DAPT:PTAA; XRD; mass; TGA; DFT.

1. INTRODUCTION

6-Aryl-2,4-diamino-1,3,5-triazines have been reported as new ligands with potential multi-coordination modes [1], cross linkers in coatings [2], vermin-micro capsules with slow-release potentiality [3], and corrosion resistant agents on metal surfaces [4]. Investigations concerning 6-substituted 2,4-diamino-1,3,5-triazine are focused in their properties in molecular recognition [5]. They also find applications as colorants [6] for making laser dyes, optical data storage devices, and liquid crystal display.

Phenylthioacetic acid (Ph-S-CH_2-COOH) is a synthetic precursor for a variety of Ph-S-containing compounds such as $PhSCH_2$ =C=O, $PhSCH_2CON$=C=S, $PhSCH_2CO_2Me$, $PhSCH_2NO_2$, MeCH=C(NO_2)SPh, $PhSCHClCO_2H$, $PhSCH_2Cl$, and 2-(phenylthio)methyl-1-oxazolidine derivatives [7-12]. Phenylthioacetic acid is used as a free radical quencher in laser flash photolysis experiments [13]. Ph-S-CH_2-COOH in its triplet excited state undergoes intermolecular electron transfer allowed by hydrogen abstraction and decarboxylation producing alkyl radicals, which are the active initiator radicals in photo-induced polymerization. Derivatives of PTAA [o-hydroxyphenylthio) acetic acid and benzal-bis-(β-thiopropionic) acid] are shown to be anti-tuberculotic [14,15]. The present work is focused on the XRD studies, spectral characteristics, and TGA of 2,4-diamino-6-phenyl-1,3,5-triazine:phenylthioacetic acid cocrystal.

2. EXPERIMENTAL

2.1 General

2,4-diamino-6-phenyl-1,3,5-triazine (DAPT) was purchased from Merk India. Phenylthioacetic acid (PTAA) was prepared by literature method [15]. Solvents were dried as per standard method. FT-IR spectra were recorded in pellet form with spectral grade KBr on a JASCO FT-IR 410 spectrometer in the range 4000–400 cm^{-1}. Single crystal XRD structure of 2,4-diamino-6-phenyl-1,3,5-triazine:phenylthioacetic acid cocrystal (DAPT:PTAA) was determined using a BRUKER APEX 2 X-ray (three-circle) diffractometer.

2.2 Synthesis of DAPT:PTAA Cocrystal

Equimolar amounts 2,4-diamino-6-phenyl-1,3,5-triazine (DAPT) and phenylthioacetic acid (PTAA) were separately prepared in dry methanol. One solution was added slowly to the other. The mixture was kept undisturbed at ambient temperature. After a period of two weeks, colorless cocrystals of DAPT:PTAA were obtained in 75% yield.

2.3 X-ray Structure

The crystal structures were determined using a BRUKER APEX 2 X-ray (three-circle) diffractometer. Intensity datasets were collected at room temperature on a BRUKER SMART APEXII CCD [16] area-detector diffractometer equipped with graphite monochromated Mo Kα radiation (λ = 0.71073 Å). The data were reduced using the program SAINT and empirical absorption corrections were carried out using the SADABS [16]. The structures were solved by direct methods using SHELXS-97 and subsequent Fourier analyses, refined anisotropically by full-matrix least-squares method using SHELXL-97 [17] within the WINGX suite of software, based on F^2 with all reflections. All carbon-hydrogen's were positioned geometrically and refined by a riding model with Uiso1.2 times that of attached atoms. All non-H atoms were refined anisotropically. The molecular structures were drawn using the ORTEP-III [18] and POV-ray [19] programs.

2.4 Computational Methodology

All calculations were performed using Gaussian 09 software [20]. Gas phase geometry was fully optimized at Density Functional Theory (DFT/B3LYP-6-31G(d)) method. The electronic properties were calculated from the Koopmans' theorem and the molecular properties like geometry, total energy, molecular electrostatic

potential, E_{HOMO}, E_{LUMO}, dipole moment, electron affinity, ionization potential, chemical potential, electronegativity, absolute hardness, softness, and nucleophilicity were carried out as reported [21].

3. RESULTS AND DISCUSSION

3.1 IR Spectra

IR spectrum was recorded to confirm the transfer of carboxylic proton from PTAA to DAPT and also to identify the specific hydrogen bonds. If a proton transfer occurs from the acid to N of the base moiety, very broad peaks would appear around 2500±100 cm^{-1}. However, absence of any such band in the IR of the cocrystal is indicative of the nontransfer of proton from the acid to the base [22]. The IR spectrum of the cocrystal shows C=O stretching frequency at 1641cm^{-1} and –OH stretching frequency at 3214 cm^{-1}. There are significant variations in the stretching frequencies of –OH, C=N, and C=O groups compared to those of the cocrystal formers. Changes in the carbonyl frequencies in the crystal [23,24], in general, indicate the formation of the cocrystal. The $C=O_{str}$ of the cocrystal (1641 cm^{-1}) shows a difference of 64 cm^{-1} from that of the free acid, PTAA (1705 cm^{-1}). Thus it is understood that the C=O group is involved in H–bonding.

3.2 Mass Spectra

The ESI mass spectrum of DAPT:PTAA in negative ion mode shows the base peak at 167.04 ($M+^{\bullet}$ of PTAA is 168.04). This indicates the loss of an amu *i.e.* a proton from PTAA forming in to anion. The mass spectrum of DAPT:PTAA cocrystal in positive ion mode shows the base peak at 188.08 ($M+^{\bullet}$ of DAPT is 187.08). This is due to the acceptance of a proton from PTAA by DAPT. Thus the protonated DAPT appears at m/z 188.08 under the mass spectral conditions.

3.3 Thermogravimetric Analysis

TGA measurement of DAPT:PTAA shows that the cocrystal remains intact until 150°C. The first weight loss of 9.9% (calc.9.85%) may be due to the elemination of one each of NH_3 and H_2O molecules at 125.8-141.3°C. The second stage decomposition of the cocrystal occurs between 160 and 270°C (66%). There is a gradual decomposition after 180°C-400°C. The cocrystal is thermally stable up to 180°C [25-28].

3.4 Single Crystal XRD Analysis of the Cocrystal DAPT:PTAA

Crystal Structure of DAPT:PTAA shows that the molecule crystallized in *Pca*2_1 space group existing as a 1:1 co-crystal. The chemical structure of DAPT:PTAA is given in Fig. 1 and ORTEP diagram and packing arrangement of the title compound are shown in Fig. 2. It consists of one molecule of 2,4-diamino-6-phenyl-1,3,5-triazine (DAPT) and one molecule of 2-phenylthioacetic acid (PTAA) in the asymmetric unit. The dihedral angle between the triazine moiety of DAPT and thioacetyl moiety of PTAA is found to be 50.89(9)°.

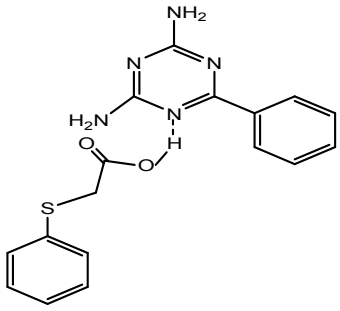

Fig. 1. The chemical structure of DAPT:PTAA

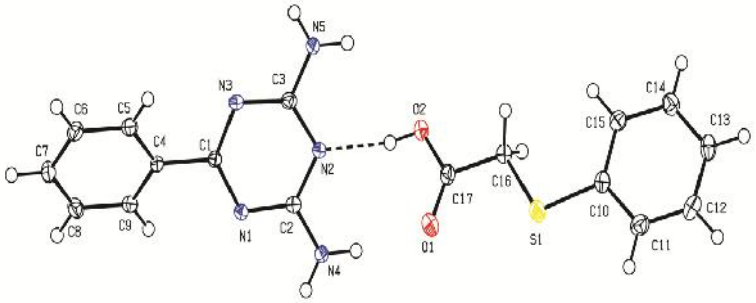

Fig. 2. ORTEP view of DAPT:PTAA with displacement ellipsoids drawn at 50% probability level

Table 1. Crystal data and structure refinement parameters for the 2,4-diamino-6-phenyl-1,3,5-triazine:phenylthioacetic acid (DAPT:PTAA) cocrystal

Empirical formula	$C_{17}H_{17}N_5O_2S$
Formula weight	355.41
Temperature	110.15 K
Wavelength	0.71073A^o
Crystal system	Orthorhombic
Space Group	P c a 21
Unit cell dimensions	a = 12.384(2) A^0 b = 18.698(3) A^0 c = 7.0428(11) A^0
Volume, V	1630.8(5) A^{o3}
Z	4
Density (calculated)	1.448 Mg/m^3
Absorption coefficient	0.221 mm^{-1}
F(000)	744
Crystal size	0.81×0.16×0.04 mm^3
Theta range for data collection	1.972 to 28.837^o
Index ranges	-16<=h<=16, -25<=k<=24, -9<=1<=9
Reflections collected	29764
Independent reflections	4111 [R(int)=0.0380]
Completeness to theta = 25.242^o	99.8 %
Absorption correction	Semi-empirical from Equivalents
Max. and Min. transmission	0.7458 and 0.7088
Refinement Method	Full-matrix-least squares F^2
Date/restraints/parameters	4111 / 1 / 227
Goodness of Fit on F^2	1.055
Final R indices [1>2sigma(I)]	R1 =0.0324, wR2 =0.0766
R indices (all data)	R1 =0.0368, wR2 =0.0796
Absolute structure parameter	0.01(2)
Extinction coefficient	n/a
Largest different peak and hole	0.387 and -0.201e.A^{o-3}

Twisting of the acid and 3° amino groups across the O–H···N hydrogen bond gives the neutral-single interaction motif as shown below [29].

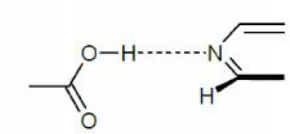

The crystal structure shows that there is no proton transfer from the carboxyl group of PTAA to the DAPT in the asymmetric unit. The predicted intermolecular hydrogen bonding motif N_2-H-O_2 is observed between the nitrogen of DAPT and carboxyl group of PTAA. It could be noticed that steric requirements warrant the H-bonding to occur between N_2 and H-O_2- and naturally the other nitrogens are spared. The crystal data collection and refinement details are presented in Table 1.

3.5 H-bondings in the Cocrystal DAPT:PTAA

Each PTAA combines with one unit of DAPT through O(2)-H(2)-N(2) hydrogen bonding with Etter's graph set designator D forming discrete molecules [30]. The O(2)---N(2) distance is 2.663Å. This bond is essentially linear, with an angle about hydrogen atom 167.0°. The normal bond length of -O-H is 0.835Å. As the carboxylic proton of PTAA forms hydrogen bonding with the N_2 of DAPT, there is a subtle increase in the bond length of the –O-H (0.84 Å) (Fig. 3).

When there is an insufficient pKa difference between the COOH and amino group, proton transfer does not occur to form any hydrogen bond such as N^+-H--$^-$O. In the cocrystal, each DAPT molecule links two different PTAA molecules through O2-H...N2 and N4-H...O1^{iii} [symmetry code: 1/2-x, y, -1/2+z] hydrogen bonds. The dihedral angle between the phenyl ring and the thioacetyl group of PTAA is found to be 11.51(11)°. The DAPT molecule forms its centro symmetric dimers *via* two pairs of N4-H...N3^i [symmetry code: -1/2+x, 1-y, z] and N5-H...N1^{ii} [symmetry code: 1/2+x, 1-y, z] hydrogen bonds with two different $R_2^2(8)$ heterosynthons [31,32] and extends as a supramolecular ribbon along the *a* axis. On each side of the supramolecular ribbon, a ring motif $R_3^3(13)$ involving one DAPT and two PTAA molecules is formed *via* N-H...O, O-H...N and weak C-H...S hydrogen bonds. The C16-H...S1^{iii} [symmetry code: 1/2-x, y, -1/2+z] hydrogen bond links symmetry related PTAA molecules. The continuous occurrence of $R_2^2(8)$ and $R_3^3(13)$ ring motifs develop two dimensional supramolecular sheet extending along *a* axis as shown in Fig. 4 The two different discrete chains C(3) formed by the primary and secondary interactions between DAPT and PTAA molecules link DAPT ribbons in the adjacent layer.

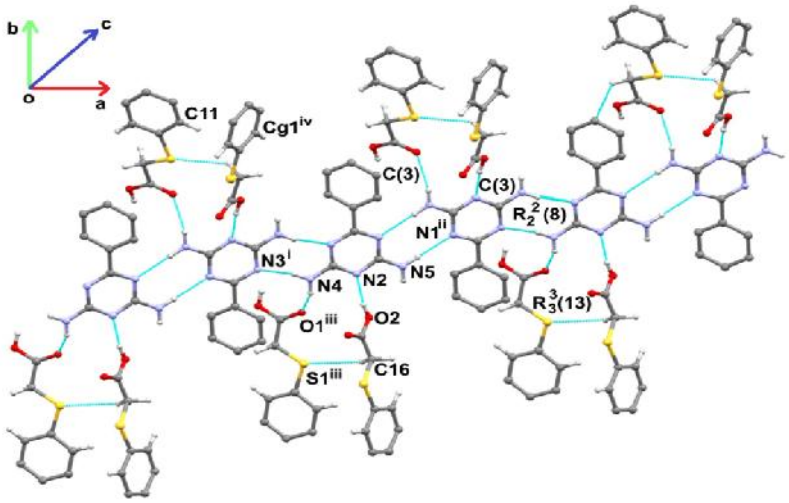

Fig. 3. Supramolecular sheets through N-H...N, N-H...O, C-H...S hydrogen bonds and C-H...π interaction. [Symmetry codes: (i) -1/2+x, 1-y, z; (ii) 1/2+x, 1-y, z; (iii) 1/2-x, y, -1/2+z; (iv) 1/2-x,y,1/2+z]

Table 2. Hydrogen bonds

D-H....A	d (D-H)	d (H...A)	d (D...A)	<(DHA)
O(2)-H(2)...N(2)	0.84	1.84	2.663(2)	167.0
N(4)-H(4A)...O(1)#1	0.88	2.21	2.985(2)	146.1
N(4)-H(4B)...N(3)#2	0.88	2.17	3.036(2)	165.9
N(5)-H(5B)...N(1)#3	0.88	2.15	3.017(2)	167.4

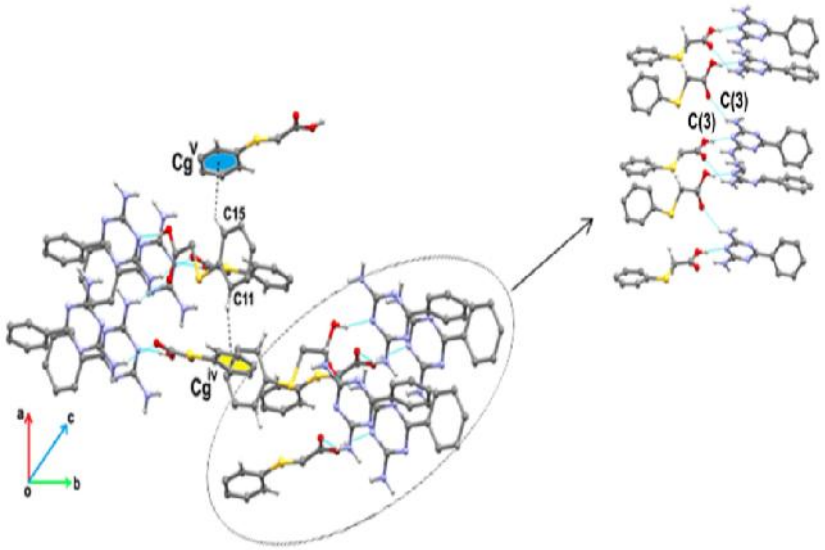

Fig. 4. Symmetry codes: 1/2-x, y, 1/2+z; (v) 1-x, -y, -1/2+z

The supramolecular sheets in adjacent layer are further connected by two different C-H...π interactions [33,34]. These weak interactions occur between phenyl C-H group (C11 and C15) of PTAA molecule and aromatic ring Cg^{iv} (symmetry code:1/2-x, y, 1/2+z) and Cg^{v} (symmetry code: 1-x, -y, -1/2+z) with d(C...π) distance of 3.642(3) and 3.510(2)Å and

d(H...π) = 2.90 and 2.72 Å, respectively (Fig. 4). The crystal structure is stabilized by the face-face π-π stacking force that is found between the parallel presence of triazine moiety of DAPT and the phenyl ring of PTAA.

3.6 Supplementary Information

The complete set of structural parameters has been deposited in CCDC (Cambridge Crystallographic Data Centre) with the CCDC deposition number 1061731. These data may be obtained free of charge from The Cambridge Crystallographic Data Centre *via* www.ccdc.cam.ac.uk/ data request/cif (or from the Cambridge Crystallographic Data Centre; Postal Address: CCDC, 12 Union Road, Cambridge CB21EZ, UK, Telephone: (44) 01223 762910, Fax: (44) 01223 336033, e-mail: deposit@ccdc.cam.ac.uk).

3.7 Theoretical Studies

The DFT method represents good correlation between the calculated geometrical parameters and the single crystal XRD (SCXRD) data. This method also helps in the calculation of the other parameters for the acid (PTAA) and the cocrystal (DAPT:PTAA). Table 3 reveals that the geometrical parameters of theoretical studies are nearly the same as the experimental ones for the acid (PTAA) and the cocrystal (DAPT:PTAA). The acid (PTAA) and the cocrystal (DAPT:PTAA) have been studied theoretically in the absence of their SCXRD data using the B3LYP/3-21G(d) level of theory. Thus we have investigated the electronic structures of the acid (PTAA) and the cocrystal (DAPT:PTAA) using the DFT method. Fig. 5 shows the optimized structures of the acid (PTAA) and the cocrystal (DAPT:PTAA). Cocrystal (DAPT:PTAA) has lower energy (-1480.18eV) than the acid (PTAA) (-621.02eV) and triazine (-853.67) (Table 3).

3.8 Frontier Molecular Orbitals

Frontier molecular orbital's (FMO) could provide information regarding the inverse dependence of stabilization energy on orbital energy difference. E_{HOMO} is generally associated with the electron donating ability of a molecule. High values of E_{HOMO} are likely to denote the tendency of the molecule to donate electrons to acceptor molecules of lower energy MO. E_{LUMO}, indicates the ability of the molecule to accept electrons [34]. The binding ability of the molecule increases with increasing HOMO and decreasing LUMO energy values. Thus, the lower the value of E_{LUMO}, the most probable it is that the molecule would accept electrons. Fig. 6 reveal the HOMO and LUMO of the cocrystal (DAPT:PTAA). From this results E_{HOMO} and E_{LUMO} value of the cocrystal is -5.6235 and -1.4171 respectively (Table 3).

The difference between the HOMO and LUMO energy levels (DE) of the molecule is an important parameter determining the reactivity of the molecule. As DE decreases (especially for the cationic species), the reactivity of the molecule increases making the molecule less stable. Table 3 reveals that the HOMO–LUMO energy gap of the cocrystal (DAPT:PTAA) is lower than that of acid (PTAA) and triazine.

The dipole moment, which is defined as the first derivative of the energy with respect to an applied electric field, is mainly used to study the intermolecular interactions such as van der Waals type dipole–dipole forces *etc*. The larger the dipole moment, the stronger will be the intermolecular attraction [35]. The cocrystal (DAPT:PTAA) has higher dipole moment (3.1456 D) which reveals it to be more polar than the acid and triazine. Absolute hardness, η, and softness, σ, are important properties to measure the molecular stability and reactivity. A hard molecule has a large energy gap and a soft molecule has a small energy gap. Soft molecules are more reactive than hard ones because they could easily offer electrons to an acceptor. For the simplest transfer of electrons, absorption could occur at the part of the molecule where σ has the highest magnitude whereas η has the lowest [36]. The nucleophilicity, ω, measures the electrophilic power of a molecule. It has been reported that the lower the value ω, the lower the capacity of the molecule to donate electrons [37]. Table 3 shows that cocrystal (DAPT:PTAA) has moderate energy gap (ΔE, 4.2064 eV).

According to the molecular orbital (MO) theory, HOMO and LUMO are the most important factors affecting the bioactivity. The interaction between these molecules and the receptor of bacteria are correlated to π–π or hydrophobic interaction among these frontier molecular orbitals. If the charged parameters are responsible for antimicrobial activity of these molecules, then the negative charges mainly located on carbonyl O-atom may be said to interact with the positive portion of the receptor. The N–H and C–H, being the most positively charged parts, can interact with the negatively charged region of the

receptor easily. We have finally resolved that the HOMO and LUMO of the cocrystal is mostly having π-antibonding type orbitals and thus, the electronic transitions from the HOMO to LUMO are mainly derived from the contribution of π–π* bands [38].

3.9 Mulliken Charge Analysis

Generally, Mulliken atomic charge calculation has an important application of quantum chemical calculations to molecular systems. It plays a vital role in the packing of crystals in the solid state by means of intermolecular interaction and it has significant influence on dipole moment, polarizability, electronic structure and vibrational modes [39]. The Mulliken charge analysis of molecules DAPT:PTAA are calculated at the HF and DFT/B3LYP levels for the molecule under study which are given in Table 4 and the corresponding population analysis graph are shown in Fig. 7.

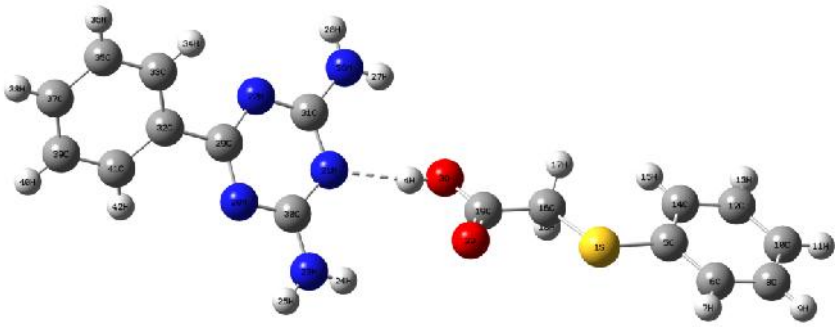

Fig. 5. Optimized structure of DAPT:PTAA

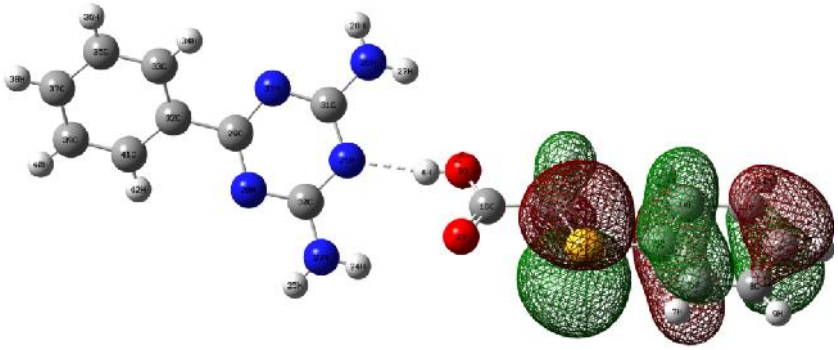

HOMO

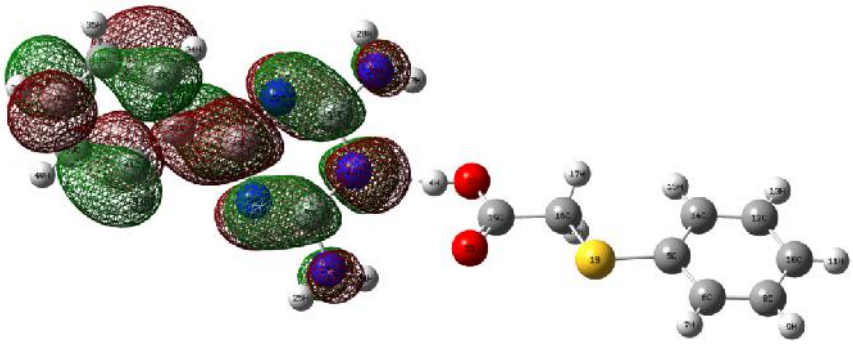

LUMO

Fig. 6. HOMO and LUMO of the cocrystal (DAPT:PTAA)

Table 3. Molecular properties of the compound calculated using DFT at the B3LYP/6-311G(d,p) basis set in gaseous phase

Compound	HOMO	LUMO	Energy gap	IP	EA	χ	μ	η	σ	(ω)	Total energy	Dipole moment
Cocrystal	-5.6235	-1.4171	4.2064	5.6235	1.4171	3.5203	-3.5203	2.1032	0.4755	2.9461	-1480.18	3.1456
Acid	-5.4921	-1.8292	3.6629	5.4921	1.8292	3.66065	-3.6606	1.83145	0.5460	3.6584	-621.02	2.8989
Triazine	-6.0163	-1.4555	4.5608	6.0163	1.4555	3.7359	-3.7359	2.2804	0.4385	3.0602	-853.67	0.1848

I – Ionization potential; A – Electron affinity; χ– Electronegativity; μ – Electrochemical potential; η – Absolute hardness; σ – Softness; ω – Nucleophilicity

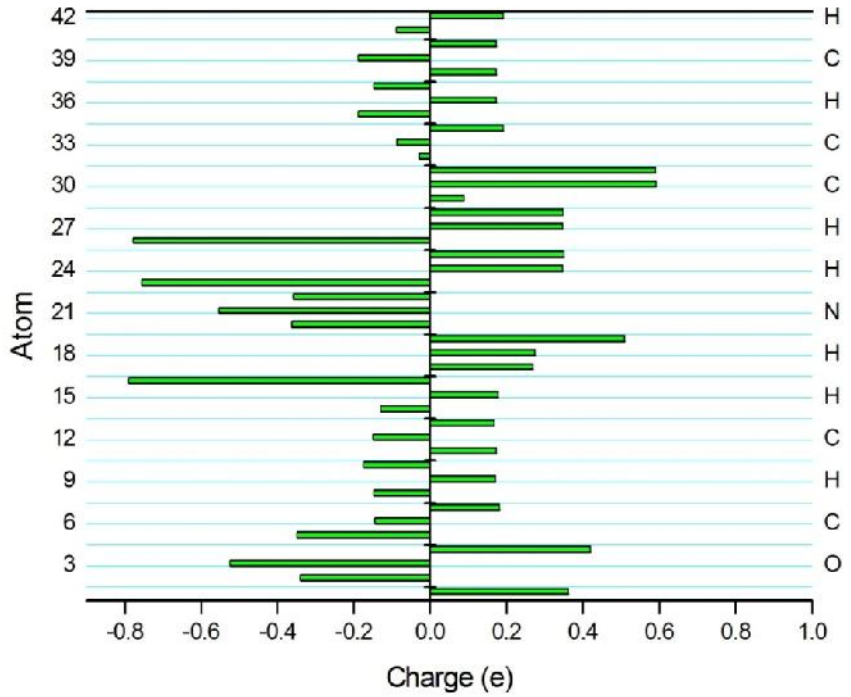

Fig. 7. Mulliken charge of DAPT:PTAA

Table 4. Mulliken charge value of cocrystal DAPT:PTAA

Atom number	Atom symbol	Mulliken charge
1	S	0.36278
2	O	-0.34062
3	O	-0.52373
4	H	0.41965
5	C	-0.34798
6	C	-0.14365
7	H	0.18155
8	C	-0.14806
9	H	0.1718
10	C	-0.17395
11	H	0.1737
12	C	-0.14951
13	H	0.16867
14	C	-0.12862
15	H	0.17883
16	C	-0.7884
17	H	0.26974
18	H	0.2748
19	C	0.50962
20	N	-0.36158
21	N	-0.55346
22	N	-0.35806
23	N	-0.75581
24	H	0.34639
25	H	0.35026
26	N	-0.77732
27	H	0.34748
28	H	0.34809
29	C	0.08845
30	C	0.59142
31	C	0.58965
32	C	-0.02729
33	C	-0.08616
34	H	0.19134
35	C	-0.18719
36	H	0.17307
37	C	-0.14785
38	H	0.17253
39	C	-0.18716
40	H	0.17287
41	C	-0.0878
42	H	0.19155

All the hydrogen atoms of DAPT:PTAA are positive nature and all nitrogen atoms are negative. Moreover, all carbon atoms have negative charges than the other four carbon atoms (C-19, C29-C31) have positive charge in nature. Because, these carbon atoms are situated between or aside the electronegative atoms (nitrogen and oxygen). This reveals the intermolecular charge transfer between the ions and hence the possibility of hydrogen bonding association and crystal packing. Especially, the intermolecular charge transfer in the two N–H···O and two N–H···N inter molecular hydrogen bonds.

4. CONCLUSION

The cocrystal 2,4-diamino-6-phenyl-1,3,5-triazine:phenylthioacetic acid (DAPT:PTAA) has been prepared. The IR(KBr) of DAPT:PTAA indicates changes in the stretching frequencies of C=O group ascertaining the formation of the cocrystal. The recorded TGA of the cocrystal shows its thermal stability upto 180°C. The ESI mass spectra indicate that proton transfer does occur under mass spectral (ESI) conditions whereas the non transfer of proton from PTAA to DAPT happens at ambient conditions (as indicated by SCXRD). Single crystal XRD of DAPT:PTAA displays the presence of a neutral-single interaction (OH…N) between the two molecules. Further the crystal structure of DAPT:PTAA is found stabilized by various H-bondings as well as π-π stackings.

ACKNOWLEDGEMENT

Authors are grateful to Prof. P. Thomas Muthiah, Head, School of Chemistry, Bharathidasan University, Tiruchirappalli-620 024, Tamilnadu, India for his assistance in XRD analysis.

COMPETING INTERESTS

Authors have declared that no competing interests exist.

REFERENCES

1. Parker B, Son DY, Silylated amino-triazines: New ligands with potential multi-coordination modes. Inorg. Chem. Commun. 2002;5:516.
2. Barclay GG, Ober CK, Papathomes KI, Wang DW. Synthesis of nanodispersible 6-aryl-2, 4-diamino-1, 3, 5-triazine and its derivatives. Macromolecules. 1992;25: 2942.
   (a) Lai SK, Batra A, Cohen C. Characterization of polydimethylsiloxane elastomer degradation via cross-linker hydrolysis, Polymer. 2005;46:4204.
   (b) Barclay GG, Ober CK, Papathomes KI, Wang DW, Synthesis of nanodispersible 6-aryl-2, 4-diamino-1, 3, 5-triazine and its

derivatives, Macromolecules. 1992;25: 2942.
3. Vikas S. Padalkar, Vikas S. Patil, Kiran R. Phatangare, Vinod D. Gupta, Prashant G. Umape, Sekar N. Synthesis of nanodispersible 6-aryl-2,4-diamino-1,3,5-triazine and its derivatives. Materials Science and Engineering. 2010;B170;77.
4. Barclay GG, Ober CK, Papathomes KI, Wang DW. Synthesis of nanodispersible 6-aryl-2, 4-diamino-1, 3, 5-triazine and its derivatives, Macromolecules. 1992;25: 2942.
5. Bing G, Yinfa Y, Huaqiang Z, Ewa SJ, Yong WK, Jin Z, Harold I. A new approach for the design of Supramolecular Recognition Units: Hydrogen-bonded molecular duplexes, J. Am. Chem. Soc. 1999;121(23):5607.
6. Lee CH, Yamamoto T. Synthesis and characterization of a new class of liquid-crystalline, highly luminescent molecules containing a 2, 4, 6-triphenyl-1, 3, 5-triazine unit, Tetrahedron Lett. 2001;42: 3993.
7. Ohshiro Y, Ando N, Komatsu M, Agawa T, Functionalized heterocumulenes: Synthesis and applications of phenylthiomethyl, methylthiomethyl, bis [phenylthio] methyl isocyanates and phenylthio-acetyl. Synthesis. 1985;276.
8. Kennedy M, McKervey MA, Maguire AR, Naughton SJ. The intramolecular Buchner reaction of aryl diazoketones. Synthesis and X-ray crystal structures of some polyfunctional hydroazulene lactones. Chem. Soc, Perkin Trans. 1990;1:1041.
9. Miyashita M, Kumazawa T, Yoshikoshi A. 1-Nitro-1-(phenylthio) propene as a new nitro olefin reagent for 3-methylfuran annulation and its application to the synthesis of some furanoterpenoids. J. Chem. Soc., Chem. Commun. 1978;362.
10. Miyashita M, Kumazawa T, Yoshikoshi A, 1-Nitro-1-(phenylthio)propene as a new nitro olefin reagent for 3-methylfuran annulation and its application to the synthesis of some furanoterpenoids. J. Org. Chem. 1980;45:2945.
11. Bordwell FG, Wolfinger JB, Dwyer JO, Solvent and substituent effects in the Ramberg-Baecklund reaction. Org. Chem. 1974;39:2516.
12. Clinet JC, Balavoine G. A novel preparative method for α, β-unsaturated oxazolines via α-phenylthiooxazolines. Tetrahedron Lett. 1987;28:5509.
13. Aydin M, Arsu N, Yagci Y, Jockusch S, Turro NJ. Mechanistic study of photoinitiated free radical polymerization using thioxanthone thioacetic acid as one-component type II photoinitiator. Macromolecules. 2005;38:4133.
14. Lange J, Urbański T. Preparation and antibacterial properties of certain derivatives of isomeric hydroxyphenylacetic acids. Dissert. Pharm. Pharmacol. 1968;20:589.
15. Solotorovsky M. Effect of ventilation on antituberculous activity of S-ethyl-L-cysteine and related compounds. Am. Rev. Tuberc. 1956;74:68.
16. Bruker APEX2, SAINT and SADABS, Bruker AXS Inc., Madison, Wisconsin, USA; 2008.
17. Sheldrick GM. A short history of SHELX. Acta Cryst. 2008;A64:112.
18. Spek AL. Structure validation in chemical crystallography. Acta Cryst. 2009;D65:148.
19. Farrugia LJ. POV-Ray – 3.5. Glasgow University, Australia; 2003.
20. Frisch MJ, Trucks GW, Schlegel HB, Scuseria GE, Robb MA, Cheeseman JR, et al. Gaussian, Inc. Wallingford, CT; 2009.
21. Suresh Kumar GS, Prabu AM, JeganJenniefer S, Bhuvanesh N, Thomas Muthiah P, Kumaresan S. Syntheses of phenoxyalkyl esters of 3, 3′-bis (indolyl) methanes and studies on their molecular properties from single crystal XRD and DFT techniques. Journal of Molecular Structure. 2013;1047:109.
22. Evans RF, Kynaston W. Hydropyrimidines. Part I. 1,4,5,6-Tetrahydropyrimidine and its derivatives. J. of the Chem. Soc. 1962; 1005.
23. Sheldrick GM. Cell_now (version 2008/1): Program for obtaining unit cell constants from single crystal data. University of Göttingen, Germany.
24. Dolomanov OV, Bourhis LJ, Gildea RJ, Howard JAK, Puschmann H, OLEX2: A complete structure solution, refinement and analysis program. J. Appl. Cryst. 2009;42:339–341.
25. Silverstein RM, Bssler GC, Morill TC, Spectrometric identification of organic compounds; 1991.
26. Preetsch P, Buhlman P, Affolter C, structure determination of organic compounds tables of spectral data; 2000.

27. Tummala M, Dhar RK, Fronczek FR, Watkins SF. 1-[3-(Naphthalen-1-yl)phen-yl]naphthal-ene. Acta Cryst. 2013; E69:o307.
28. Otwinowski Z, Minor W. Methods in enzymology, macromolecular crystallography. Part A, edited by C. W. Carter Jr. & R. M. Sweet, Academic Press. 1997; 276:307.
29. Altomare A, Burla MC, Camalli M, Cascarano GL, Giacovazzo C, Guagliardi A, Moliterni AGG, Polidori G, Spagna RJ. OLEX1: A complete structure solution, refinement and analysis program. J. Appl. Cryst. 1999;32:115–119.
30. Sheldrick GM. SHELXL97. University of Gottingen, Germany; 1997.
31. Farrugia LJ. Structure and characterization of N-(2-hydroxy-1-naphthylidene) threonine. Appl. Cryst. 1999;32:837.
32. Etter MC. Hydrogen bonds as design elements in organic chemistry. J. Phys. Chem. 1991;95:4601.
33. Wang J, Xiang, Wu A, Eng X, Robust R 2 2 (8) hydrogen bonded dimer for crystal engineering of glycoluril derivatives. Cryst Eng Comm. 2013;1510079.
34. Gomathi S, Muthiah PT. 2-Amino-4,6-di-methyl-pyrimidine–sorbic acid (1/1). Acta Crys. 2013;69:1235.
35. Ahamad I, Prasad R, Quraishi MA. Mater, anticorrosion potential of 2-Mesityl-1Himidazo[4,5-f][1,10]phenanthroline on mild steel in sulfuric acid solution: Experimental and theoretical study. Chem. Phys; 2010. Available:http://dx.doi.org/10.1016/j.matchemphys.2010.08.051
36. Bouklah M, Harek H, Touzani R, Hammouti B, Harek Y. Experimental and quantum chemical characterization of the adsorption of some Schiff base compounds of phthaloyl thiocarbohydrazide on the mild steel in acid solutions. Arab. J. Chem. Available:http://dx.doi.org/10.1016/j.arabjc.2010.08.008
37. Obi-Egbedi NO, Obot IB. Anticorrosion Potential of 2-Mesityl-1H-imidazo[4,5-f][1,10]phenanthroline on mild steel in sulfuric acid solution: Experimental and theoretical study. Ind. Eng. Chem. Res. 2011;50(4):2098.
38. Masoud MS, Awad MK, Shaker MA, El-Tahawy MMT. The role of structural chemistry in the inhibitive performance of some aminopyrimidines on the corrosion of steel. Corros. Sci. 2010;52:2387.
39. Sidir I, Sidir YG, Kumalar M, Tasal E. Synthesis, molecular structure, spectroscopic analysis, thermodynamic parameters and molecular modeling studies of (2-methoxyphenyl) oxalate. J. Mol. Struct. 2010;964:134.

Peer-review history:
The peer review history for this paper can be accessed here:
http://prh.sdiarticle3.com/review-history/20138